Flexible Magnetic Filaments as Micromechanical Sensors

C. Goubault

Laboratoire Colloïdes et Matériaux Divisés, UMR 7612, ESPCI, 10 rue Vauquelin, 75005 Paris, France and Laboratoire Physico-Chimie Curie, Institut Curie, UMR 168, 26 Rue d'Ulm, 75005 Paris, France

P. Jop and M. Fermigier

Laboratoire Physique et Mécanique des Milieux Hétérogènes, UMR 7636, ESPCI, 10 Rue Vauquelin, 75005 Paris, France

J. Baudry, E. Bertrand, and J. Bibette

Laboratoire Colloïdes et Matériaux Divisés, UMR 7612, ESPCI, 10 rue Vauquelin, 75005 Paris, France

(Received 24 March 2003; revised manuscript received 2 July 2003; published 30 December 2003)

We propose a new micromechanical approach to probe bending rigidity at molecular scale. Long flexible filaments made of magnetic colloids and linkers are shown to adopt under magnetic field a hairpin configuration. Measuring the hairpin curvature as a function of the field intensity and the linker length from diffracted light allows us to deduce the linker bending rigidity κ. The technique is presented for two types of linkers: a spontaneously adsorbing polymer and a grafted biomolecular.

DOI: 10.1103/PhysRevLett.91.260802 PACS numbers: 07.10.Cm, 07.10.Pz, 82.37.Rs

Superparamagnetic colloids have been used for several years for widely different applications: applying very small forces [1] or torques [2] to DNA molecules, directly measuring colloidal force-distance profiles [3], targetting and isolating biomolecules or cells [4], and, more recently, separating large DNA fragments [5]. Here, we describe a novel type of magnetic material: long flexible filaments made of assembled submicronic superparamagnetic colloids, which combine the elastic properties of wormlike chains and the expected response to an external field. Indeed, under a magnetic field, these filaments adopt a multiple hairpin metastable configuration which depends on their length and on the bending rigidity of linkers. The linker structure may vary from a single adsorbed macromolecule to a more complex biological sandwiched architecture. As a first application of these assembled structures, we describe a novel technique to probe the bending rigidity of these various types of molecular linkers. This technique broadens the range of micromechanical measurements focused on bending modes, beyond direct fluctuation analysis [6] or optical tweezer techniques [7].

The magnetic filaments are obtained by combining the self-assembling ability of dipolar colloids and the ability to control the formation of permanent links with field intensity [8,9]. Using this method, filaments longer than 200 μm with various kinds of linkers can be made. The curvature of the hairpins can be reversibly controlled by the field intensity. The bending rigidity of a single molecular linker can be deduced from the dependence of this curvature on field intensity, and from the linker length which can be measured optically [3].

One example of such flexible magnetic filaments is shown in Fig. 1. They are made from monodisperse superparamagnetic colloidal particles (radius $a = 375$ nm) supplied by Ademtech [10], linked by spontaneously adsorbed polyacrylic acid (PAA, Mw = 250 000, Sigma). The particles are first suspended at a volume fraction $\phi = 0.1\%$, in an aqueous solution containing 0.1% in weight of PAA and 0.1% in weight of nonyl phenol ethoxylate (surfactant NP10, Sigma). The suspension is introduced into a thin cell with a thickness of $e = 200$ μm, and subjected to a magnetic field perpendicular to the cell surface. Upon application of the field, the induced dipole moment in each particle leads to aggregation of the particles into filaments, one particle thick, with a length equal to the cell thickness [11]. Applying a sufficiently strong field (25 mT) causes the PAA molecules to irreversibly link particles [8]. After removing the field, the chains bend under their own weight, as seen in Fig. 1.

The mechanism of sticking involves the bridging of adsorbed polymers on adjacent particles. At large interparticular distances (larger than the radius of gyration R_G), the colloidal force is repulsive and scales as $\exp(-r/R_G)$ [12]. At shorter distances, imposed by the magnetic field, the process of bridging can occur and allows the chains to persist. The distance at which this

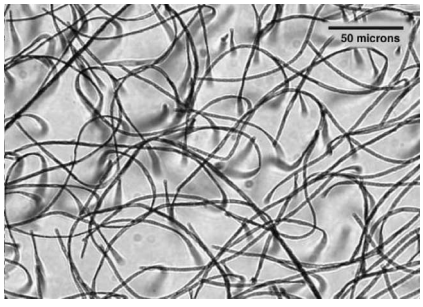

FIG. 1. Long flexible monodisperse filament, seen from above, made in a 200 μm thick cell. The chains are bent by gravity after field removal.

bridging takes place is less than R_G and corresponds to a colloidal force of tens of pN. This rather high force threshold is responsible for the perfect alignment of particles within each chain: Indeed, this threshold can be reached only when the particles are perfectly aligned as a result of the angular dependence of dipolar interactions.

The PAA linked filaments exhibit a magnetoelastic response and are chosen to illustrate this new phenomenology. To properly observe it, chains of various lengths, from 10 to 100 μm, are allowed to sediment to the bottom of the cell. Then, the chains are oriented and the field is switched off [Fig. 2(a)], then switched on again after a rotation of 90° [Figs. 2(b) and 2(c)]. Depending on the chain length, we observe three distinct behaviors. Short chains bend slightly and then rotate to align with the new field direction. Longer chains bend into hairpin shapes, with two straight ends aligned with the field, separated by a curved section. Still longer chains can form multiple bends. When the magnetic field is removed, curved chains return within a few seconds to a nearly straight configuration, a result of the stored elastic energy. We also checked that over rather short times (a few minutes to 1 h after preparation) this behavior remained unchanged, revealing the persistence of these elastic properties.

The equilibrium shape of the hairpins results from a balance between the magnetic force which tends to align the two ends of the chain with the field direction and the elastic force resisting bending. This coupling is evidenced in Fig. 3: The hairpin curvature increases linearly with the applied field.

Since the deformation is localized only within the links, the hairpin radius of curvature R is related to the radius of curvature of the linker R_p through the geometrical relation $R_p = R(l/2a)$, where l is the linker length [see Fig. 4 (left)]. If we assume that the bending rigidity of the linker is κ, the elastic energy stored within one link is $U_{\rm el} = \kappa l/R_p^2$. At equilibrium, the total elastic energy of the filament (sum of elastic energy for all links) is balanced by the total magnetic energy, which is the sum of all dipole-dipole interactions [13]. This magnetic energy has the scaling $U_m \propto \mu_0 \chi^2 H^2 a^3$, where χ is the effective magnetic susceptibility of the particles and μ_0 the vacuum permeability. Balancing $U_{\rm el}$ and U_m yields the expected linear relation between the curvature of the chain, $1/R$, and the applied field H:

$$\frac{1}{R} \propto \chi H \sqrt{\frac{\mu_0 a l}{4\kappa}}. \tag{1}$$

To get an accurate measurement of the chain flexibility and linker rigidity, we model the filaments as continuous elastic fibers and derive analytically their shape as a function of magnetic field strength [14]. The computed shapes agree with the experiments and confirm that a single elastic constant, the bending rigidity κ, is sufficient to account for the deformation. This calculation, in the limit of long hairpins (i.e., with a length much larger than the radius of curvature), gives the maximum dimensionless curvature of the chain as $C_{\rm max} = 2a/R$:

$$C_{\rm max} = \chi H \sqrt{\frac{\pi \mu_0 a^3 l}{6\kappa}}. \tag{2}$$

To evaluate the bending rigidity κ at the scale of a single link, the length l should also be measured. The particle spacing h is determined from collecting the Bragg diffracted light of the oriented chain under the magnetic field, which allows direct scanning of colloidal force-distance profile [3]. We first measure this profile in the

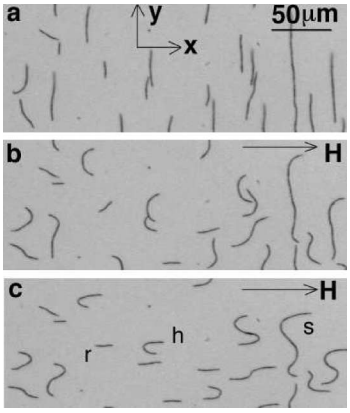

FIG. 2. Orientation dynamics of polydisperse chains. (a) Filaments are first sedimented on the bottom of the cell and aligned in the y direction; (b) 2 s after a 90° (x direction) rotation of the field ($H = 1000$ A/m); (c) 10 s after field rotation. Short chains rotate as almost rigid rods (r). Longer chains form hairpins (h). Still longer chains bend into sinuous shapes (s).

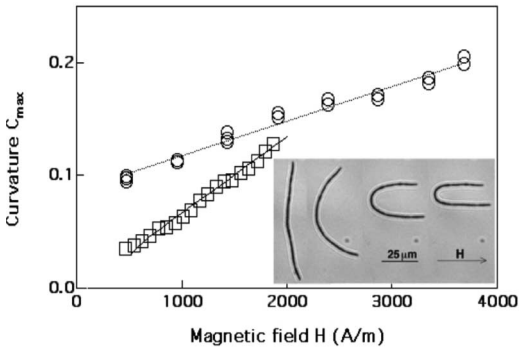

FIG. 3. Maximum dimensionless curvature ($2a/R$) of the hairpin as a function of the magnetic field. Squares: experimental results for PAA ($a = 375$ nm). Solid line: computation with $\kappa = 7.8 \times 10^{-26}$ J/m (see text). Circles: experimental results for vWF ($a = 103$ nm). Dotted line: computation with $\kappa = 1.5 \times 10^{-26}$ J/m. Inset: equilibrium hairpin shapes for PAA linked particles ($a = 375$ nm), field increasing from 200 to 1800 A/m.

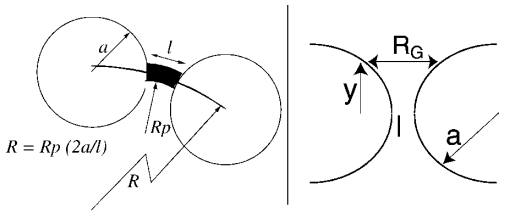

FIG. 4. Left: Geometrical relation between the chain radius of curvature R and the radius of curvature of the linker R_p. Right: Definition of the linker width y as a function of particle diameter a and R_G. For the purpose of clarity, the linker and the particles are not drawn to scale.

absence of linker and deduce the hard core diameter h_c. We then repeat this measurement in the presence of linkers [8] and determine the distance h at which the chains remain permanently intact after the field is switched off. The difference $h - h_c$ directly measures the linker length l. For adsorbed PAA, Mw = 250 000, we found $l = 10 \pm 5$ nm, which is less than the radius of gyration $R_g = 35$ nm, as expected. By fitting the data of Fig. 3 with Eq. (2), the bending modulus associated with these bridging polymers is found to be $\kappa = 7.8 \times 10^{-26}$ J m ($\kappa/l = 7.8 \times 10^{-18}$ J $\approx 2000 k_B T$). The high bending energy found for this type of spontaneously adsorbed linker clearly suggests the existence of many bridges made of distinct loops, in agreement with adsorbed polymer theory [15]. Indeed, a flexible polymer, with a similar mass, grafted only at its ends, would give a negligible bending rigidity.

We assume that the linker consists of a rod of length l and radius y, at which the distance between the curved surfaces exceeds R_G [Fig. 4 (right)]. Indeed, on average, spontaneous stretching beyond R_G is very unlikely. This radius y is such that $y^2 = aR_G - la$. The bending rigidity is related to y by $\kappa = E\pi y^4/4$, where E is the Young's modulus of this effective rod. In our experiment, $y \approx 95$ nm and $\kappa = 7.8 \times 10^{-26}$ J m, leading to $E \approx 1 \times 10^3$ Pa. In a polymer gel, $E \approx k_B T/\xi^3$, where ξ is the average distance between reticulation points. By comparing with our measurement, we deduce $\xi \approx 15$ nm, which is equal to the distance between particle surfaces l. Therefore the elasticity of these confined polymers can be simply related to the average distance between immobilized segments, as in a gel. In other words, the adsorption onto colloidal surfaces constrains the motion of the polymer as reticulation points would do.

Before generalizing this technique to other linkers, we examine the limiting curvature of the hairpins that can be reached before the colloidal surfaces come into contact. If the curvature is too high, the particles will touch and stretch the linker, precluding any reliable bending measurement. This limiting (dimensionless) curvature $C = 2a/R$ is such that $1 - C^2/4 = (1 - l/2a)^2$. For the beads used here, the limiting curvature is $C = 2a/R = 0.32$, whereas the maximum curvature experienced by the PAA linkers was 0.1. Therefore, our measurements probe only a bending mode.

Many other types of linkers may be explored through this new technique, particularly those having biological implications. As an example, we explore the rigidity of an antibody/antigen sandwich: IgG–vWF–IgG. The von Willebrand factor (vWF Calibrator, Diagnostica Stago) is a multimeric plasma glycoprotein involved in primary hemostasis and in the coagulation process [16]. Its molecular weight ranges from 520 000 up to 10^7. The immunoglobulin G (IgG, Corgenix Inc.) is a rabbit anti-human vWF. The biomechanics of vWF is important because its deformation under blood flow-induced shear stress is thought to regulate platelet adhesion [17]. The von Willebrand factor can specifically recognize two IgG, as it is commonly employed to measure vWF concentration in human plasma, with latex agglutination immunoassays [16]. Using recommended standard procedures, IgG is directly grafted onto magnetic particles of radius 103 nm [18]. In the presence of vWF, these particles immediately link into chains under a magnetic field whereas the agglutination is much slower in the absence of field. Because of the low density of grafted IgG onto the particles (less than 1 IgG per 2000 nm^2), the number of molecular complexes per link is close to 1. In addition, the kinetics of destruction of the chains in the absence of field is single exponential. Therefore the measured rigidity refers to one single complex per link on average.

In Fig. 5, we report colloidal force-distance profiles in various conditions to measure the linker length. In the absence of a linker, the force-distance curve allows one to deduce the hard core diameter h_c which is very close to

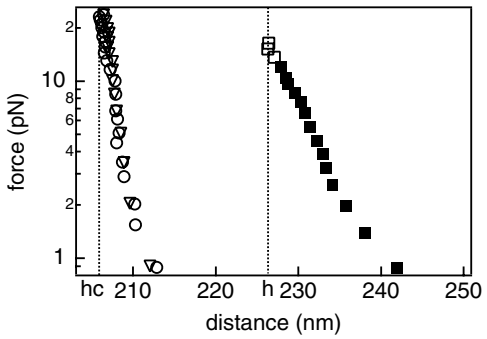

FIG. 5. Measurement of the colloidal force (pN) as a function of the distance (nm) deduced from Bragg diffraction. The particle diameter is 206 nm [10]. Open circles: carboxylic particles in phosphate buffer 10 mM pH = 7; open triangles: anti-vWF IgG grafted particles in phosphate buffer 10 mM pH = 7; solid squares: in the presence of the linker (vWF), open squares correspond to the case where the chains remain permanent after the field is switched off. h_c: hard core diameter; h: distance at which the chains remain permanent after the field is switched off.

the particle diameter given by the manufacturer. In the presence of an appropriate amount of linker (about half the grafted protein concentration), we find a long range repulsive force and a threshold both for the force and the distance h at which linking takes place within a few seconds. Although we do not yet have an explanation for the origin of the long range repulsion, we can build these permanent chains by overtaking this barrier which ensures, as for the PAA linker, the formation of perfectly aligned chains. The linker length is the difference $h - h_c$.

From both the plot of the curvature as a function of the magnetic field and the optical measurement of the linker length $l = 20 \pm 5$ nm (Fig. 5), we deduce $\kappa = 1.5 \times 10^{-26}$ J m and $\kappa/l = 200 k_B T$ (Fig. 3). We note that the curvature does not extrapolate to zero for zero field. This effect is due to residual friction of the chain on the bottom surface of the cell, which imposes the existence of a threshold magnetic energy to overtake this friction. This effect is much less visible for the previous example because of its much higher bending rigidity. However, the relatively high rigidity of the sandwich rules out a simple random coil-like behavior of the vWF. This large mass protein should thus be viewed as a compact and cohesive structure within the immunological complex.

As shown on the basis of these two selected examples, this technique can probe the rigidity of a variety of linkers and particularly those having biological importance. Moreover, the better understanding of the micromechanical properties of molecules offers new insight into their structural properties. Finally, we believe that single molecule biomechanics can also take advantage of this simple approach.

We thank Jean-Louis Viovy, Jacques Prost, David Pine, and Carlos Marques for fruitful discussions. We acknowledge the technical help of Catherine Rouzeau, Rémi Dreyfus, Anne Koenig, Caroline Derec, and Patrice Jenffer, and financial support from the French Ministère de la Recherche.

[1] S. B. Smith, L. Finzi, and C. Bustamante, Science **258**, 1122 (1992).
[2] T. R. Strick, J.-F. Allemand, D. Bensimon, A. Bensimon, and V. Croquette, Science **271**, 1835 (1996).
[3] F. L. Calderon, T. Stora, O. M. Monval, P. Poulin, and J. Bibette, Phys. Rev. Lett. **72**, 2959 (1994).
[4] D. Newman and C. Price, *Principles and Practice of Immunoassay* (MacMillan Reference, London, 1997), Chap. 8.
[5] P. S. Doyle, J. Bibette, A. Bancaud, and J.-L. Viovy, Science **295**, 2237 (2002).
[6] A. Ott, M. Magnasco, and A. Simon, Phys. Rev. E **48**, R1642 (1993).
[7] E. Furst and A. Gast, Phys. Rev. Lett. **82**, 4130 (1999).
[8] J. Philip, O. Mondain-Monval, F. L. Calderon, and J. Bibette, J. Phys. D **30**, 2798 (1997).
[9] E. M. Furst, C. Suzuki, M. Fermigier, and A. P. Gast, Langmuir **14**, 7334 (1998).
[10] http://www.ademtech.com. These particles are obtained from controlled emulsification of octane based ferrofluid. Octane is further extracted and each particle is finally composed of 40% in volume of iron oxide. They are stabilized by sodium dodecyl sulfate which is replaced for the purpose of our experiment by a mixture of PAA and NP10, through a washing procedure.
[11] J. Liu, E. Lawrence, A. Wu, M. Ivey, G. A. Flores, K. Javier, J. Bibette, and J. Richard, Phys. Rev. Lett. **74**, 2828 (1995).
[12] O. Mondain-Monval, A. Espert, P. Omarjee, J. Bibette, F. Leal-Calderon, J. Philiip, and J.-F. Joanny, Phys. Rev. Lett. **80**, 1778 (1998).
[13] H. Zhang and M. Widom, Phys. Rev. E **51**, 2099 (1995).
[14] In the continuum model, the energy of the curved filament is

$$U = \int_{-L/2}^{L/2} \left[EI\left(\frac{d\theta}{ds}\right)^2 + \frac{4\pi\mu_0}{72} a^3 \chi^2 H^2 \frac{(1 - 3\cos^2\theta)}{2a} \right] ds,$$

where s is the curvilinear abscissa along the chain, L is the filament length, $\theta(s)$ is the angle between the filament and the magnetic field, and EI is the apparent bending rigidity of the filament. EI is related to the rigidity κ and length l of the elastic linker through $EI = \kappa(2a/l)$. We normalize the magnetic and elastic energies by the thermal energy, introducing the persistence length $\lambda_p = EI/k_B T$ and b_H, the ratio of the energy of interaction of two beads aligned with the field to $k_B T$. The minimization of U leads to a differential equation for the shape of the hairpin: $\theta'^2 - c_H f(\theta) = C_0$, where $\theta' = d\theta/ds'$, $c_H = b_H(a/\lambda_p)$, and $f(\theta) = 1 - 3\cos^2\theta$, with $s = s/2a$ being the dimensionless curvilinear abscissa and C_0 a constant determined by the boundary conditions. The shape of the hairpins is found by solving this differential equation with $\theta = \pi/2$ in the middle of the filament and a vanishing curvature at the free ends. For filaments of finite length, we solve the differential equation numerically and compute the maximum curvature in the middle of the chain. For very long filaments, there is an analytic expression of the maximum curvature [Eq. (2)].
[15] A. Semenov and J. Joanny, Europhys. Lett. **29**, 279 (1995).
[16] F. Jobin, *L'hémostase* (Les Presses de l'Université Laval, Sainte-Foy, Quebec, 1995).
[17] J. Sadler, Annu. Rev. Biochem. **67**, 395 (1998).
[18] http://www.ademtech.com. These particles are first obtained as the previous ones, but surface polymerization is used to control the density of carboxylic groups on the surface. IgG is directly grafted onto carboxylic groups.